Synthesis, Molecular Structure, and Stereochemical Nonrigidity of Bis(3-(dimethylamino)propyl)difluorostannane Dihydrate, $\{[Me_2N(CH_2)_3]_2SnF_2\cdot 2H_2O\}$, and Enhanced Reactivity of Its Fluoride Adduct $\{[Me_2N(CH_2)_3]_2SnF_3\}^-Bu_4N^+$ toward Dichloromethane†

Nicole Pieper,‡ Carmen Klaus-Mrestani,§ Markus Schürmann,‡ and Klaus Jurkschat*,‡

Chair for Inorganic Chemistry II, University of Dortmund, Otto-Hahn-Strasse 6, D-44227 Dortmund, Germany, and Department of Biochemistry/Biotechnology, Martin Luther University Halle-Wittenberg, Weinbergweg 16a, D-06099 Halle/S., Germany

Monique Biesemans, Ingrid Verbruggen, José C. Martins, and Rudolph Willem*

High Resolution NMR Centre (HNMR), Free University of Brussels (VUB), Pleinlaan 2, B-1050 Brussel, Belgium

Received October 22, 1996⊗

The X-ray diffraction analysis of crystals of $\{[Me_2N(CH_2)_3]_2SnF_2\cdot 2H_2O$ (**3a**) obtained by reaction of $[Me_2N(CH_2)_3]_2SnR_2$ (R = Me, Ph) with Pr_3SnF reveals a six-coordinate, distorted octahedral geometry at tin with the pairs of fluorine, nitrogen and carbon atoms bound to the metal atom being all in a mutual *trans* configuration. Room-temperature ^{119}Sn, ^{19}F, ^1H, and ^{13}C NMR spectra of **3a** reveal exchange averaging with loss of the $^1J(^{119}Sn-^{19}F)$ coupling on the ^{119}Sn and ^{19}F NMR time scales. Below −50 °C, ^{119}Sn and ^{19}F NMR coupling data evidence the existence of only two isomers among the five *a priori* possible ones, a major (*ca.* 80%) and a minor species (*ca.* 20%). The methyl ^{13}C resonance as well as the $^1J(^{119}Sn-^{19}F)$, $^1J(^{119}Sn-^{13}C)$, and $^2J(^{19}F-^{13}C)$ coupling patterns reveal the major species to have the same *all-trans* structure as in the crystal state, while the minor species has a *cis* arrangement for its fluorine and nitrogen atoms and the *trans* one for its carbon atoms. Gradient assisted $^1H-^{119}Sn$ HMQC spectroscopy establishes $^3J(^{119}Sn-^1H)$ correlations through the $Me_2N\rightarrow Sn$ bond to exist in both slow- and fast-exchange ranges. Together with the loss of the $^1J(^{119}Sn-^{19}F)$ coupling at high temperature, this evidences the $Me_2N\rightarrow Sn$ coordination to be maintained during the *cis*−*trans* isomerization and the latter to occur through a dissociative mechanism involving tin−fluorine bond rupture. Addition of $Bu_4N^+F^-\cdot 3H_2O$ in CH_2Cl_2 yields under quaternization of one nitrogen zwitterionic $\{[Me_2(ClCH_2)N^+(CH_2)_3][Me_2N(CH_2)_3]SnF_3^-\}\cdot H_2O$ (**3b**).

Introduction

Octahedral diorganotin compounds of types A−C (Chart 1) are known for a long time.[1] Their structure was intensively studied by means of multinuclear NMR and Mössbauer spectroscopy and by X-ray analysis. This is not only due to pure academic interest but also due to the anticancer activity shown in recent years, at least when screened *in vitro*.[2]

Most of the compounds studied show a *trans*-SnR_2 skeleton with the X and D ligands in *cis* positions. *cis*-SnR_2 arrangements were only reported for $Me_2Sn(quin)_2$[3] and $Me_2Sn(ONHCOMe)_2$.[4] For $(4\text{-}ClC_6H_4)_2SnCl_2\cdot$4,4-Me$_2$bipy both the *cis*- and *trans*-SnR_2 skeletal isomers are known.[1e] In solution they seem to undergo rapid interconversion. *All-trans*-configurated octahedral diorganotin species are reported for $Me_2SnCl_2\cdot 2D$ (D = Py,[5a] 3,5-dimethylpyrazole-*N*-2,[5b] 2(1*H*)-pyridinethione-*S*,[5c] *N*-methylimidazole,[5d] 2,6-$(Me_2NCH_2)_2C_6H_3SnI_2(4\text{-}MeC_6H_4)$, and $(Me_2NCH_2CH_2CMe_2)_2SnCl_2$[5f]). In solution *cis-trans* equilibria in inorganic hexacoordinate tin complexes of types A−C are generally fast on the ^1H NMR time scale. We are aware of only one report tentatively describing the observation of different iso-

† Dedicated to Professor Herbert Jacobs on the occasion of his 60th birthday.
‡ University of Dortmund.
§ Martin Luther University.
⊗ Abstract published in *Advance ACS Abstracts,* February 1, 1997.

(1) (a) Kumar Das, V. G.; Chee-Keong, Y.; Smith, P. J. *J. Organomet. Chem.* **1987**, *327*, 311 and references cited therein. (b) Jastrzebski, J. T. B. H.; van Koten, G. *Adv. Organomet. Chem.* **1993**, *35*, 241. (c) Howard, W. F.; Crecely, R. W.; Nelson, W. H. *Inorg. Chem.* **1985**, *24*, 2204. (d) Jurkschat, K.; Kalbitz, J.; Dargatz, M.; Kleinpeter, E.; Tzschach, A. *J. Organomet. Chem.* **1988**, *347*, 41. (e) Kumar Das, V. G.; Keong, Y. C.; Wei, C.; Smith, P. J.; Mak, T. C. W. *J. Chem. Soc., Dalton Trans.* **1987**, 129 and references cited therein.

(2) (a) Caruso, F.; Gianini, M.; Giuliani, A. M.; Rivarola, E. *J. Organomet. Chem.* **1994**, *466*, 69 and references cited therein. (b) Crowe, A. J. In *Metal Complexes in Cancer Chemotherapy*; Keppler, B. K., Ed.; VCH: Weinheim, Germany, 1993; p 369−379. (c) Gielen, M.; Lelieveld, P.; de Vos, D.; Willem, R. In *Metal Complexes in Cancer Chemotherapy*; Keppler, B. K., Ed.; VCH: Weinheim, Germany, 1993; p 381−390. (d) Gielen, M.; Lelieveld, P.; de Vos, D.; Willem, R. Metal-Based Drugs. In *Metal-Based Antitumour Drugs*; Gielen, M., Ed.; Freund Publishing House: Tel Aviv, Israel, 1992; Vol. 2, p 29−54.

(3) Schlemper, E. O. *Inorg. Chem.* **1967**, *6*, 2012.

(4) Harrison, P. G.; King, T. J.; Phillips, R. C. *J. Chem. Soc., Dalton Trans.* **1976**, 2317.

S0276-7333(96)00895-3 CCC: $14.00

Chart 1

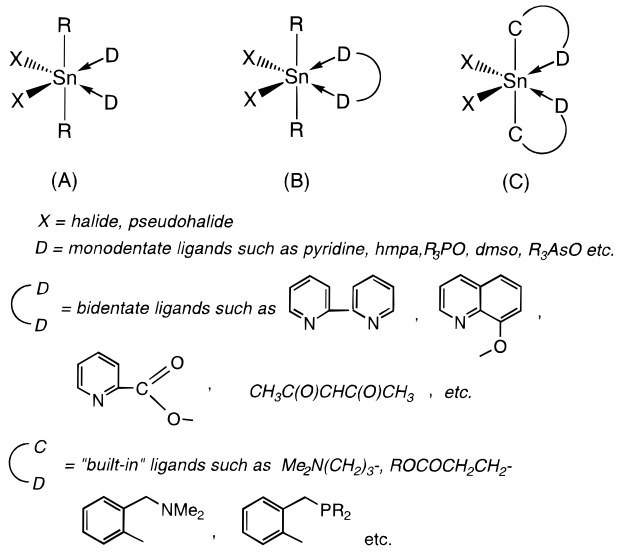

mers of octahedral diorganotin compounds in solution.[6] This is somewhat surprising but may be traced to the usually poor solubility of hexacoordinate organotin compounds making low-temperature NMR studies difficult if not impossible.

This was for instance the case for $[Me_2N(CH_2)_3]_2SnCl_2$ (**1**), a compound we synthesized some years ago. Its ^{119}Sn NMR spectrum displays a single resonance at −184.7 ppm. The half-width of this signal of about 215 Hz made us suspicious about a possible dynamic process taking place in this derivative.

Although organotin fluorides usually exhibit very poor solubility, we and others have shown that introducing bulky substituents,[7] adding fluoride,[8] or making intramolecular coordination[9] possible provides highly soluble systems.

Replacing the chlorine atoms in **1** by fluorine would give $[Me_2N(CH_2)_3]_2SnF_2$, a model compound easy to study by NMR spectroscopy because of the additional NMR-active ^{19}F nuclei. As shown below, **3** was isolated as its water adduct $\{[Me_2N(CH_2)_3]_2SnF_2 \cdot 2H_2O\}$, hereafter referred to as **3a**.

Our main investigation tools for the elucidation of the solution structure and dynamic stereochemistry of **3a**, as well as its coordination behavior toward the fluoride anion, were ^1H, ^{13}C, ^{119}Sn, ^{19}F 1D NMR, and gradient-assisted[10] $^1H-^{119}Sn$ heteronuclear multiple quantum correlation (HMQC) spectroscopy[11,12] as well as ^{19}F-detected $^{19}F-^{117}Sn$ HMQC spectroscopy applied, to the best of our knowledge, for the first time to this pair of nuclei by the method of Berger[13] using two spectrometers. For solid-state measurements, ^{13}C and ^{117}Sn CP-MAS NMR was applied.[14,15]

Experimental Section

General Considerations. All solvents were dried by standard procedures. IR spectra were recorded on a Bruker IFS 28 spectrometer. Molecular weight measurements were performed on a Knauer osmometer. The electrospray mass spectrum was obtained using a VG Quattro II.

Synthesis of Bis(3-(dimethylamino)propyl)tin Dichloride, $[Me_2N(CH_2)_3]_2SnCl_2$ (1). The Grignard reagent $Me_2N(CH_2)_3MgCl$, prepared from $Me_2N(CH_2)_3Cl$ (40 g, 0.33 mol) and magnesium (7.9 g, 0.3 mol) in 200 mL of THF was added dropwise at −40 °C to a mechanically stirred solution of $SnCl_4$ (41.7 g, 0.16 mol) in 150 mL of THF. The color changed to reddish-brown. After 2 h, the external cooling was removed and the reaction mixture was refluxed for 1 h. The THF was distilled off under reduced pressure, and 400 mL of toluene was added to the residue. The resulting mixture was again refluxed for 10 min under mechanical stirring followed by filtration of the hot mixture in order to remove the insoluble magnesium salt. The filtrate was evaporated *in vacuo*, and the residue was recrystallized from dry methanol to yield 36.9 g (63.6 %) of **1**, mp 245 °C.

Anal. Found: C, 33.53; H, 6.73; N, 7.67; Cl, 18.78. Calcd for $C_{10}H_{24}Cl_2N_2Sn$ (361.92): C, 33.19; H, 6.68; N, 7.74; Cl, 19.59.

^1H NMR ($CDCl_3$): $SnCH_2$, 1.63 ppm (m, 4H); CH_2, 2.09 ppm (m, 4H); NCH_2, 2.72 ppm (m, 4H); NMe, 2.65 ppm (s, 6H). ^{13}C NMR ($CDCl_3$): $SnCH_2$, 31.0 ppm, $^1J(^{119}Sn-^{13}C) = 903$ Hz; CH_2, 21.2 ppm, $^2J(^{119}Sn-^{13}C) = 60$ Hz; NCH_2, 59.5 ppm, $^3J(^{119}Sn-^{13}C) = 87$ Hz; NMe, 47.3 ppm. ^{119}Sn NMR ($CDCl_3$): −184.7 ppm.

Synthesis of Bis(3-(dimethylamino)propyl)dimethyltin, $[Me_2N(CH_2)_3]_2SnMe_2$ (2). Method A. A diethyl ether solution of MeMgCl (0.08 mol) was added under magnetic stirring to a suspension of **1** (10 g, 0.03 mol) in 200 mL of diethyl ether. The reaction mixture was refluxed for 2 h, cooled to 0 °C, and hydrolyzed with a saturated aqueous ammonium chloride solution, and the aqueous layer was extracted with ether using a perforator. The combined ether layers were dried over Na_2SO_4. After filtration of the Na_2SO_4 and evaporation of the ether, the residue was distilled *in vacuo* to give 6 g (67 %) of **2** as a colorless oil, bp 120 °C (0.07 Torr).

(5) (a) Ashlanov, L. A.; Ionov, V. M.; Attiya, V. M.; Pernin, A. B.; Petrosyan, V. S. *Zh. Strukt. Khim.* **1978**, *19*, 185. (b) Graziani, R.; Casellato, U.; Ettore, R.; Plazzogna, G. *J. Chem. Soc., Dalton Trans.* **1982**, 805. (c) Valle, G.; Ettore, R.; Vettori, U.; Peruzzo, V.; Plazzogna, G. *J. Chem. Soc., Dalton Trans.* **1987**, 815. (d) Bardi, R.; Piazzesi, A.; Ettore, R.; Plazzogna, G. *J. Organomet. Chem.* **1984**, *270*, 171. (e) Jastrzebski, J. T. B. H.; van der Schaaf, P. A.; Boersma, J.; de Wit, M.; Wang, Y.; Heijdenrijk, D.; Stam, C. H. *J. Organomet. Chem.* **1991**, *407*, 301. (f) Schollmeyer, D.; Hartung, H.; Klaus, C.; Jurkschat, K. *Main Group Met. Chem.* **1991**, *14*, 27.

(6) Pettinari, C.; Rafaiani, G.; Lobbia, G. G.; Lorenzotti, A.; Bonati, F.; Bovio, B. *J. Organomet. Chem.* **1991**, *405*, 75.

(7) (a) Al-Juaid, S.; Dhaher, S. M.; Eaborn, C.; Hitchcock, P. B.; Smith, J. D. *J. Organomet. Chem.* **1987**, *325*, 117. (b) Reuter, H.; Puff, H. *J. Organomet. Chem.* **1989**, *379*, 223.

(8) (a) Dakternieks, D.; Zhu, H. *Organometallics* **1992**, *11*, 3820. (b) Dakternieks, D.; Zhu, H. *Inorg. Chim. Acta* **1992**, *196*, 19. (c) Dakternieks, D.; Jurkschat, K.; Zhu, H.; Tiekink, E. R. T. *Organometallics* **1995**, *14*, 2512.

(9) (a) Dostal, S.; Stoudt, S. J.; Fanwick, P.; Sereaton, W. F.; Kahr, B.; Jackson, J. E. *Organometallics* **1993**, *12*, 2284. (b) Kolb, U.; Dräger, M.; Dargatz, M.; Jurkschat, K. *Organometallics* **1995**, *14*, 2827. (c) Preut, H.; Godry, B.; Mitchell, T. N. *Acta Crystallogr.* **1992**, *C48*, 1994. (d) Kolb, U.; Dräger, M.; Jousseaume, B. *Organometallics* **1991**, *10*, 2737. (e) Ochiai, M.; Iwaki, S.; Ukita, T.; Matsuura, Y.; Shiro, M.; Nagao, Y. *J. Am. Chem. Soc.* **1988**, *110*, 4606.

(10) (a) Keeler, J.; Clowes, R. T.; Davis, A. L.; Laue, E. D. *Methods Enzymol.* **1994**, *239*, 145. (b) Tyburn, J.-M.; Bereton, I. M.; Doddrell, D. M. *J. Magn. Reson.* **1992**, *97*, 305. (c) Ruiz-Cabello, J.; Vuister, G. W.; Moonen, C. T. W.; Van Gelderen, P.; Cohen, J. S.; Van Zijl, P. C. M. *J. Magn. Reson.* **1992**, *100*, 282. (d) Vuister, G. W.; Boelens, R.; Kaptein, R.; Hurd, R. E.; John, B. K.; Van Zijl, P. C. M. *J. Am. Chem. Soc.* **1991**, *113*, 9688. (e) Willem, R.; Bouhdid, A.; Kayser, F.; Delmotte, A.; Gielen, M.; Martins, J. C.; Biesemans, M.; Tiekink, E. R. T. *Organometallics* **1996**, *15*, 1920.

(11) (a) Bax, A.; Griffey, R. H.; Hawkins, B. H. *J. Magn. Reson.* **1983**, *55*, 301. (b) Bax, A.; Summers, M. F. *J. Magn. Reson.* **1986**, *67*, 565.

(12) Kayser, F.; Biesemans, M.; Gielen, M.; Willem, R. *J. Magn. Reson. A* **1993**, *102*, 249.

(13) (a) Berger, S. *J. Fluorine Chem.* **1995**, *72*, 117. (b) Berger, S.; Wetzel, N. *TAMU-NMR Newslett.* **1994**, 12. (c) Marion, D.; Wüthrich, K. *Biochem. Biophys. Res. Commun.* **1983**, *113*, 967.

(14) Bovey, F. A.; Jelinski, L; Mirau, P. A. *Nuclear Magnetic Resonance Spectroscopy*, 2nd ed.; Academic Press Inc.: San Diego, CA, 1987; Chapter 8, pp 399−434.

(15) Sebald A. MAS and CP/MAS NMR of Less Common Spin-1/2 Nuclei. In *Solid State NMR II: Inorganic Matter*; Diehl, P., Fluck, E., Günther, H., Kosfeld, R., Seelig, J., Eds.; Springer Verlag: Berlin, 1994; p 91.

Anal. Found: C, 45,42; H, 9.51; N, 8.51. Calcd for $C_{12}H_{30}N_2Sn$ (321.09): C, 44.89; H, 9.42; N, 8.72.

^{1}H NMR ($CDCl_3$): SnMe, −0.16 ppm (s, $^2J(^{119}Sn-^1H) = 51$ Hz, 6H); $SnCH_2$, 0.58 ppm (m, 4H); CH_2, 1.45 ppm (m, 4H); NCH_2, 2.10 ppm (m, 4H); NMe, 2.0 ppm (s, 6H). ^{13}C NMR ($CDCl_3$): SnMe, −11.3 ppm ($^1J(^{119}Sn-^{13}C) = 435$ Hz); $SnCH_2$, 7.7 ppm ($^1J(^{119}Sn-^{13}C) = 349$ Hz); CH_2, 24.7 ppm ($^2J(^{119}Sn-^{13}C) = 19$ Hz; NCH_2, 63.7 ppm ($^3J(^{119}Sn-^{13}C) = 57$ Hz); NMe, 45.5 ppm. ^{119}Sn NMR ($CDCl_3$): −0.1 ppm.

Method B. Dimethyltin dichloride (10 g, 0.046 mol) was dissolved in 100 mL of THF and added dropwise to a magnetically stirred solution of $Me_2N(CH_2)_3MgCl$, prepared from $Me_2N(CH_2)_3Cl$ (11.1 g, 0.091 mol) and magnesium (2.3 g, 0.095 mol) in 80 mL of THF. The reaction mixture was refluxed for 2 h, and subsequently the THF was distilled off. Diethyl ether (100 mL) was added, and the mixture was hydrolyzed under ice cooling with water (100 mL). The ether layer was separated and the water layer was extracted twice with 50 mL of diethyl ether. The combined organic layers were dried over Na_2SO_4, filtered, and evaporated. Distillation gave 10.6 g (72%) of **2**.

Synthesis of Bis(3-(dimethylamino)propyl)diphenyltin, $[Me_2N(CH_2)_3]_2SnPh_2$ (2a). This compound was obtained according to method B from $Me_2N(CH_2)_3Cl$ (12 g, 0.098 mol), magnesium (2.4 g, 0.098 mol), and Ph_2SnCl_2 (14 g, 0.041 mol) as a slightly yellow oil (14.8 g, 81%), bp 120 °C (0.001 Torr).

Anal. Found: C, 60.26; H, 7.72; N, 6.47. Calcd for $C_{22}H_{34}N_2Sn$ (445.24): C, 59.35; H, 7.70; N, 6.29. ^{1}H NMR ($CDCl_3$): SnPh, 7.29, 7.46 (m, 10H); $SnCH_2$, 1.24 ppm (m, 4H); CH_2, 1.76 ppm (m, 4H); NCH_2, 2.22 ppm (m, 4H); NMe, 2.11 ppm (s, 6H). ^{13}C NMR (C_6D_6): $SnCH_2$, 8.4 ppm ($^1J(^{119/117}Sn-^{13}C) = 382/366$ Hz); CH_2, 24.8 ppm ($^2J(^{119/117}Sn-^{13}C) = 20$ Hz, satellites unresolved); NCH_2, 63.3 ppm ($^3J(^{119/117}Sn-^{13}C) = 53$ Hz, satellites unresolved); NMe, 45.6 ppm; C(ipso), 141.7 ppm ($^1J(^{119/117}Sn-^{13}C) = 437/418$ Hz); C(ortho), 137.1 ppm ($^2J(^{119/117}Sn-^{13}C) = 33$ Hz, satellites unresolved); C(meta), 128.5 ppm ($^3J(^{119/117}Sn-^{13}C) = 44$ Hz, satellites unresolved); C(para), 128.5 ppm. ^{119}Sn NMR ($CDCl_3$): −73 ppm.

Synthesis of Bis(3-(dimethylamino)propyl)tin Difluoride Water Adduct $[Me_2N(CH_2)_3]_2SnF_2 \cdot 2H_2O$ (3a). Bis(3-(dimethylamino)propyl)dimethylstannane, $[Me_2N(CH_2)_3]_2SnMe_2$ (3.76 g, 12 mmol), and tri-*n*-propyltin fluoride, Pr_3SnF (6.25 g, 23 mmol), were heated for 30 min to 150 °C resulting in a clear melt. After cooling to room temperature chloroform was added and the resulting solution was stirred for 5 min. Traces of unreacted *n*-Pr_3SnF were filtered off. The chloroform was evaporated *in vacuo*, ether was added to the residue, and the mixture was stirred for 5 min. The colorless precipitate was carefully filtered off and recrystallized from toluene to give 2.6 g (68%) of **3a**, mp 152 °C.

Molecular weight determination (osmometrically in C_6H_6): found, 347 g/mol.

Anal. Found: C, 32.55; H, 7.31; N, 7.52. Calcd for $C_{10}H_{28}F_2N_2O_2Sn$ (365.05): C, 32.90; H, 7.73; N, 7.67. Mass spectrum: *m/e* 330 ($C_{10}H_{24}F_2N_2Sn^+$), 311 ($C_{10}H_{24}FN_2Sn^+$), 288 ($C_7H_{18}F_2N_2Sn^+$), 244 ($C_5H_{12}F_2NSn^+$), 225 ($C_5H_{12}FNSn^+$), 206 ($C_5H_{12}NSn^+$), 139 (SnF^+). IR (Nujol): ν_{OH} 3308, 3438, 3485 cm^{-1}.

Synthesis of $\{[Me_2(ClCH_2)N^+(CH_2)_3][Me_2N(CH_2)_3]SnF_3^-\} \cdot H_2O$ (3b). Bis(3-(dimethylamino)propyl)tin difluoride water adduct $[Me_2N(CH_2)_3]_2SnF_2 \cdot 2H_2O$ (0.22 g, 0.6 mmol) and $Bu_4NF \cdot 3H_2O$ (0.575 g, 1.82 mmol) were dissolved in 15 mL of dichloromethane. The reaction mixture was refluxed for 1 h and stirred overnight. The precipitate formed was filtered off and dried to give 0.19 g (82%) of **3b**, mp 165−167 °C. Anal. Found: C, 31.30; H, 7.00; N, 6.62. Calcd for $C_{11}H_{28}ClF_3N_2OSn$ (415.51): C, 31.80; H, 6.79; N, 6.74.

IR (Nujol): ν_{OH} 3408, 3439 cm^{-1}.

ESMS in methanol (positive mode): *m/e* 379, $\{[Me_2(ClCH_2)N^+(CH_2)_3][Me_2N(CH_2)_3]SnF_2\}^+$.

Crystallography. Crystals of **3a** were grown from toluene by slow evaporation. Intensity data for the colorless crystal were collected with $\omega/2\theta$ scans on a Nicolet R3m/V diffractometer with graphite-monochromated Mo Kα radiation. The lattice parameters were determined from a symmetry-constrained least-squares fit of the angular settings for 37 reflections with $2\theta_{max} = 24.4°$. Six standard reflections were recorded every 300 reflections, and an anisotropic intensity loss up to 2.8% was detected during X-ray exposure. The data were corrected for Lorentz−polarization decay but not for absorption effects. Systematic absences (hkl) $h + k = 2n+1$, ($h0l$) $h = 2n + 1$, and ($0k0$) $k = 2n + 1$ were detected. The structure was solved by standard Patterson and difference Fourier methods with SHELXTL PLUS[16] (Sheldrick, 1987) and refined satisfactorily with space group *C*2/*m* (No. 12) by full-matrix least-squares calculations with SHELXL93.[17] The H atoms were placed in geometrically calculated positions and refined with a common isotropic temperature factor for the methyl and methylene groups (H_{methyl}, C−H 0.98 Å, $H_{methylene}$, C−H 0.97 Å; $U_{iso(all)}$ 0.111(16) Å^2). Two methylene groups C(2) and C(3) are disordered and refined with an sof value of 0.5. Atomic scattering factors for neutral atoms and real and imaginary dispersion terms were taken from ref 16. The programs used were SHELXTL PLUS,[17] SHELXL93,[18] PARST,[19] PLATON,[20] and MISSYM.[21] Crystallographic data are given in Table 1, and positional parameters and equivalent values of the anisotropic displacement parameters for the non-H atoms are given in the Supporting Information.

Table 1. Crystallographic Data for 3a

empirical formula	$C_{10}H_{24}F_2N_2Sn \cdot 2H_2O$
fw	365.03
temp	291(1) K
wavelength	0.710 69 Å
cryst system	monoclinic
space group	*C*2/*m* (No. 12)
unit cell dimens	$a = 10.966(13)$ Å, $\alpha = 90°$ $b = 8.475(6)$ Å, $\beta = 122.91(8)°$ $c = 9.797(12)$ Å, $\gamma = 90°$
V	764.4(14) Å^3
Z	2
D(calcd)	1.586 Mg/m^3
D(measd)	1.656(3) Mg/m^3
abs coeff	1.688 mm^{-1}
F(000)	372
cryst size	0.32 × 0.30 × 0.24 mm
θ range for data collcn	2.48−25.06°
index ranges	$0 < h < 13$, $-1 < k < 10$, $-11 < l < 9$
reflcns collcd	860
indepdt reflcns	724 [*R*(int) = 0.0172]
refinement method	full-matrix least-squares on F^2
data/restraints/param	724/0/56
goodness-of-fit on F^2	1.091
final *R* indices	$R1 = 0.0484$ ($F > 4\sigma(F)$); $wR2 = 0.1121$ (F^2)
largest diff peak and hole	1.396 and −1.546 e Å^{-3}

NMR Experiments. Solid State. All CP-MAS NMR spectra[14] were recorded on a Bruker AC250 spectrometer, operating at 89.15 and 62.93 MHz for ^{117}Sn and ^{13}C nuclei, respectively. The spectrometer is interfaced with an Aspect 3000 computer and equipped with a MAS broad-band probe for solid-state experiments. The matching condition for Hartmann−Hahn cross-polarization[14] (^{1}H 90° pulse length: 5 ms) was set with (c-$C_6H_{11})_4Sn$ for the ^{117}Sn nucleus, as well as the chemical shift reference (−97.35 ppm relative to $(CH_3)_4Sn$);[15] adamantane was used (38.3 ppm relative to $(CH_3)_4Si$) for the

(16) *International Tables for Crystallography*; Kluwer Academic Publishers: Dordrecht, The Netherlands, 1992; Vol. C.
(17) Sheldrick, G. M. SHELXTL-PLUS. Release 3.4 for Nicolet R3m/V crystallographic system. An Integrated System for Solving, Refining and Displaying Crystal Structures from Diffraction Data. Nicolet Instrument Corporation, Madison, WI, 1987.
(18) Sheldrick, G. M. University of Göttingen, 1993.
(19) Nardelli, M. *Comput. Chem*. **1983**, *7*, 95.
(20) Spek, A. L. *Acta Crystallogr*. **1990**, *A46*, C34
(21) Le Page, Y. *J. Appl. Crystallogr*. **1987**, *20*, 264−69.

^{13}C nucleus. ZrO_2 rotors (7 mm o.d.) and a spinning rate of 4 kHz were used for the ^{13}C acquisitions. The ^{13}C spectrum was obtained by acquiring 4K data points over a spectral width of 19.2 kHz, a 1.5 ms contact time, and a relaxation delay of 4 s with 1000 scans. The ^{117}Sn spectra were typically obtained by acquiring 32K data points over a spectral width of 166.7 kHz, a 2 ms contact time, and a relaxation delay of 2 s with 5000 scans. In order to find the isotropic chemical shift, spectra were run at three different spinning rates[14] (5000, 4500, and 3900 Hz).

^{117}Sn spectra were recorded instead of the more common ^{119}Sn ones to overcome a local radio interference problem on the AC250 Bruker instrument of the VUB.[22] No misinterpretations are to be expected when comparing solution or solid state ^{117}Sn and ^{119}Sn chemical shift data, since $^{117}Sn/^{119}Sn$ isotopic effects on tin chemical shifts are known to be negligible.[23]

NMR Experiments. Solution State. The NMR spectra were recorded on a Bruker AMX500 spectrometer interfaced with a X32 computer and operating at 500.13, 125.77, and 186.50 MHz for the ^1H, ^{13}C, and ^{119}Sn nuclei, respectively. The ^{19}F NMR spectra as well as some routine spectra were acquired on a Bruker AC250 instrument equipped with a Quattro probe tuned to 250.13, 62.93, 89.15, and 235.19 MHz for ^1H, ^{13}C, ^{117}Sn, and ^{19}F nuclei, respectively. ^1H and ^{13}C chemical shifts were referenced to the standard Me_4Si scale from respectively residual ^1H and $^{13}C-^2H$ solvent resonances (CD_2Cl_2, 5.32 and 53.6 ppm; CCl_4/C_6D_6, 7.15 and 128.0 ppm for ^1H and ^{13}C nuclei, respectively). The ^{119}Sn and ^{117}Sn reference frequencies were calculated from the absolute ^1H frequency of TMS and the known absolute frequency of Me_4Sn, being respectively $\Xi(^{119}Sn) = 37.290\ 665$ MHz and $\Xi(^{117}Sn) = 35.632\ 295$ MHz[24] at the B_0 field where the absolute frequency of the ^1H nucleus is exactly 100.000 000 MHz. For ^{19}F nuclei, the reference was $CFCl_3$, with $\Xi(^{19}F) = 94.094\ 003$ MHz.[24b]

^{13}C and ^{119}Sn BB proton-decoupled 1D spectra were recorded using standard pulse sequences and delays from the Bruker program library.

The proton-detected 1D and 2D $^1H-^{119}Sn$ HMQC correlation spectra with or without ^{119}Sn decoupling were acquired using the pulse sequences of the Bruker program library,[11] adapted to include gradient pulses,[10] as described recently.[10e] The resulting improvement in spectrum quality, due to optimal artifact suppression, has been outlined elsewhere.[10e] For evidencing specifically the long-range correlation between ^1H *N*-methyl resonances and the ^{119}Sn resonances, the experiments were optimized to an average $^nJ(^1H-^{119}Sn)$ value of the order of 4 Hz (delay = 120 ms). No low-pass *J* filter was applied.[11b]

The fluorine-19-detected 2D $^{19}F-^{117}Sn$ HMQC correlation spectra were acquired without ^{117}Sn decoupling using the resources of two NMR spectrometers, in a "master-slave" relationship, as described recently by Berger for $^{19}F-^{13}C$ nuclei pairs.[13] ^{19}F acquisition was performed on the AC250 instrument with the ^1H coil of the QNP probe being tuned to the ^{19}F resonance frequency. ^{117}Sn pulses were generated on the AMX500 instrument under direct control of the AC250 one and sent to the X-coil of the QNP probe. The concentration of **3a** in CD_2Cl_2 was 63 mM. The $^{19}F-^{117}Sn$ HMQC spectra were acquired in 14 min at 233 K, in the phase sensitive mode using TPPI,[13c] with 2048 data points in t_2, 16 time increments in t_1, a relaxation delay of 1 s, and 16 scans preceded by 4 dummy scans for each FID. Processing consisted of zero filling to 128 points in F1, multiplication by a $\pi/2$ shifted squared sinebell in both dimensions, Fourier transformation, and magnitude calculation in F2.

Scheme 1

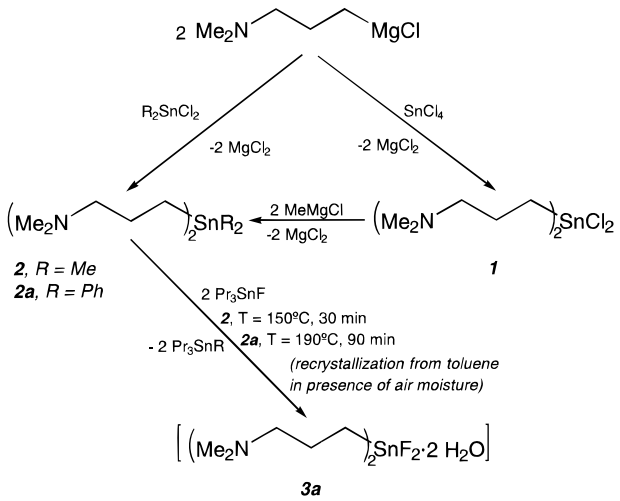

Results and Discussion

Synthetic Aspects. Organotin fluorides are usually prepared by treatment of organotin halides (halogen = Cl, Br, or I) with aqueous solutions of potassium fluoride, exploiting the usually poor solubility of the resulting organotin fluorides in both water and common organic solvents such as CH_2Cl_2, ether, or acetone. However, this method does not apply to $[Me_2N(CH_2)_3]_2SnF_2$ as this compound was not expected to be insoluble. In fact, it is soluble in CH_2Cl_2 and even in water.

Compound **3** was prepared in good yield as its water adduct **3a** by reaction of $[Me_2N(CH_2)_3]_2SnR_2$ (**2,** R = Me; **2a,** R = Ph) with Pr_3SnF and subsequent recrystallization from toluene in the presence of air moisture (Scheme 1).

The driving force for this reaction is the formation of the intramolecular N→Sn coordination in **3a**, as shown previously for similar compounds.[9] Compounds **2** and **2a** were prepared directly from the corresponding diorganotin dichloride and $Me_2N(CH_2)_3MgCl$. **2** was also obtained by methylation of bis(3-(dimethylamino)-propyl)tin dichloride (**1**). The latter compound was obtained in good yield by reaction of tin tetrachloride with $Me_2N(CH_2)_3MgCl$. It is interesting to note that when the phenyl derivative **2a** was used in the reaction with Pr_3SnF, a higher temperature and a longer reaction time were required. This contradicts earlier findings according to which tin−phenyl bonds are easier to be cleaved than tin−methyl bonds.[25] We tentatively attribute our result to steric reasons.

Molecular Structure of 3a. The molecular structure of **3a** is shown in Figure 1, and selected bond lengths and bond angles are summarized in Table 2.

The tin atom in **3a** shows slightly distorted *all-trans* octahedral configuration. The only distortion from the ideal geometry arises from the C(1)−Sn(1)−N(1) and C(1)−Sn(1)−N(1a) angles of 81.9(4) and 98.1(4)°, respectively; it can be attributed to some strain in the five-membered $NSnC_3$ ring. Thus the structure resembles

(22) (a) Koch, B. R.; Fazakerley, G. V.; Dijkstra, E. *Inorg. Chim. Acta* **1980**, *45*, L51. (b) Harrison, P. G. *Chemistry of Tin*; Harrison, P. G., Ed.; Blackie & Son Limited: Glasgow, U.K., 1989; Chapter 3, p 113.

(23) McFarlane, H. C. E.; McFarlane, W.; Turner, C. J. *Mol. Phys.* **1979**, *37*, 1639.

(24) (a) Davies, A. G.; Harrison, P. G.; Kennedy, J. D.; Puddephatt, R. J.; Mitchell, T. N.; McFarlane, W. *J. Chem. Soc. A* **1969**, 1136. (b) Mason, J. *Multinuclear NMR*; Plenum Press: New York, 1987; pp 625−629.

(25) Abraham, M. H.; Grellier, P. L. *The Chemistry of the Metal-Carbon Bond*; Hartley, F. R., Patai, S., Eds.; Wiley & Sons: London, **1985**; Vol. 2, p 25.

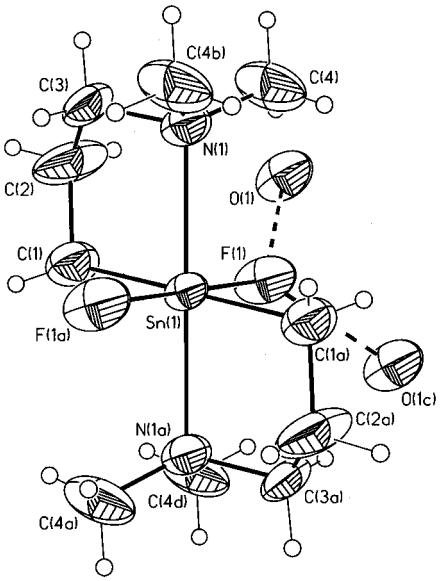

Figure 1. General view (SHELXTL-PLUS) of a molecule of **3a** showing 50% probability displacement ellipsoids and the atom numbering. (Symmetry transformations used to generate equivalent atoms: (a) $-x, -y, -z$; (b) $x, -y, z$; (c) $-x, -y + 1, -z$; (d) $-x, y, -z$).

Table 2. Selected Interatomic Bond Distances (Å) and Angles (deg) for 3a[a]

Bond Distances			
Sn(1)−F(1)	2.084(6)	Sn(1)−N(1)	2.366(8)
Sn(1)−C(1)	2.112(11)	F(1)−O(1)	2.805(7)
Bond Angles			
F(1a)−Sn(1)−F(1)	180.0	O(1)−F(1)−O(1c)	79.7(3)
F(1)−Sn(1)−C(1)	90.0	C(2)−C(1)−Sn(1)	107.7(8)
C(1a)−Sn(1)−C(1)	180.0	C(3)−C(2)−C(1)	112(5)
F(1)−Sn(1)−N(1)	90.0	C(2)−C(3)−N(1)	109(2)
C(1a)−Sn(1)−N(1)	98.1(4)	C(4)−N(1)−C(4b)	107.9(9)
C(1)−Sn(1)−N(1)	81.9(4)	C(4)−N(1)−C(3)	126.9(8)
N(1)−Sn(1)−N(1a)	180.0	C(4b)−N(1)−C(3)	96.6(7)
Sn(1)−F(1)−O(1)	140.1(2)	C(4)−N(1)−Sn(1)	111.8(5)
Sn(1)−F(1)−O(1c)	140.1(2)	C(3)−N(1)−Sn(1)	100.8(6)

[a] Symmetry transformations used to generate equivalent atoms: (a) $-x, -y, -z$; (b) $x, -y, z$; (c) $-x, -y + 1, -z$.

very much those of its chlorine-substituted analogue $[Me_2N(CH_2)_3]_2SnCl_2$,[5f,26] $(Me_2NCH_2CH_2CMe_2)_2SnCl_2$,[5f] and the compounds cited in ref 5. The Sn−N distance of 2.366(8) Å exceeds the sum of the covalent radii of tin and nitrogen (2.10 Å) and reflects a Pauling type bond order[27] of about 0.73. It is shorter than the corresponding Sn−N bonds in $[Me_2N(CH_2)_3]_2SnCl_2$[5f] (2.403(3) Å) and $[Me_2NCH_2CH_2CMe_2]_2SnCl_2$[5f] (2.448(4) Å) and also in $N(CH_2CH_2CH_2)_3SnF \cdot H_2O$[9b] (2.426(6), 2.393(5) Å).

The Sn−F bond length of 2.084(6) Å is shorter than the corresponding distances reported for Me_2SnF_2[28] (2.12(1) Å) and $(NH_4)_2(Me_2SnF_4)$[29c] (2.121(5), 2.126(3), 2.135(4) Å), the only other structurally characterized diorganotin difluorides and diorganotin tetrafluoride dianions, respectively. The lengthening of the Sn−F distance in **3a** compared to a single Sn−F bond length of 1.96 Å[7b] is a result of intramolecular Sn−N coordination and hydrogen bridging to the water molecules. This effect has previously been reported for $N(CH_2CH_2CH_2)_3SnF \cdot H_2O$.[9b]

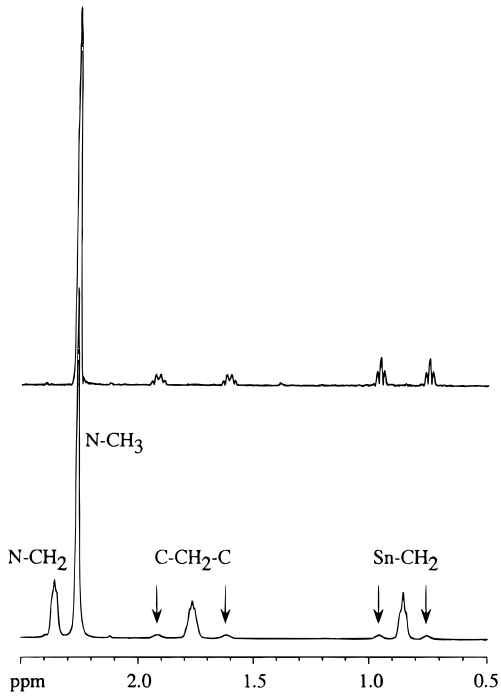

Figure 2. Gradient-assisted 1D $^1H-^{119}Sn$ HMQC spectrum (top) of a CCl_4/C_6D_6 solution of $[Me_2N(CH_2)_3]_2SnF_2 \cdot 2H_2O$ (**3a**). Delay: 120 ms. Assignment of the different ^{119}Sn edited ^1H nuclei is given. A standard 1D NMR spectrum is given for comparison (bottom). Arrows in the standard 1D spectrum indicate the $^nJ(^1H-^{119}Sn)$ coupling satellites edited in the 1D $^1H-^{119}Sn$ HMQC spectrum (top). The HMQC spectrum has been Fourier transformed in the magnitude mode.

1D NMR Data. ^1H and ^{13}C NMR data for compound **3a** are collected in Table 3. At room temperature and above, the ^1H spectra reveal the expected resonances, though broad and without $^nJ(^1H-^1H)$ coupling resolution (Figure 2, bottom). This suggests the existence of a dynamic process in the intermediate to fast-exchange range on the proton NMR scale. Chemical shifts and coupling constants are essentially solvent independent, being similar in CCl_4/C_6D_6 (~9/1), CD_2Cl_2, and C_5D_5N. Unresolved broad $^nJ(^1H-^{119/117}Sn)$ coupling satellites are visible for the CH_2Sn and the $C-CH_2-C$ methylene protons only. Lowering the temperature results in resonance splitting, confirming chemical exchange between different species.

Room-temperature ^{13}C spectra acquired from CD_2Cl_2 solutions reflect fast-exchange averaging, with no $^nJ(^{13}C-^{19}F)$ coupling being visible.

Low-temperature ^{13}C spectra reveal the existence of two species, a major one **M** (*ca.* 80%) and a minor one **m** (*ca.* 20%). The $^1J(^{13}C-^{119/117}Sn)$ coupling constants of 1060/1010 Hz for the major species **M** are very similar to the average coupling of 1030 Hz found in the CP/MAS ^{13}C spectrum (Table 3). This suggests the major solution species **M** to be identical to the one observed

(26) Schollmeyer, D. PhD Thesis, Martin Luther University Halle-Wittenberg, 1989.
(27) Kolb, U.; Beuter, M.; Dräger, M. *Inorg. Chem.* **1994**, *33*, 4522.
(28) Schlemper, E. O., Hamilton, W. C. *Inorg. Chem.* **1966**, *5*, 995.
(29) (a) Kayser, F.; Biesemans, M.; Bouâlam, M.; Tiekink, E. R. T.; El Khloufi, A.; Meunier-Piret, J.; Bouhdid, A.; Jurkschat, K.; Gielen, M.; Willem, R. *Organometallics* **1994**, *13*, 1098. (b) Tiekink E. R. T. *Appl. Organomet. Chem.* **1991**, *5*, 1. (c) Tudela, D. *J. Organomet. Chem.* **1994**, *471*, 63.

Table 3. ^{1}H and ^{13}C NMR Data for $[Me_2N(CH_2)_3]_2SnF_2\cdot 2H_2O$[a] (3a)

moieties	chem shift	coupling constants
	^{1}H NMR (333 K; CCl_4/C_6D_6)	
CH_2Sn	0.85[b]	$^{2}J(^{1}H-^{119}Sn) = 105$[c]
$C-CH_2-C$	1.77[b]	$^{3}J(^{1}H-^{119}Sn) = 154$[c]
CH_2N	2.36[b,d]	
CH_3N	2.26[e]	$^{3}J(^{1}H-^{119}Sn) < 3$[f]
	*1*H NMR (213 K; CD_2Cl_2)	
CH_2Sn	0.85 (**M**); 1.0−1.3 (**m**)[g,h]	$^{2}J(^{1}H-^{119/117}Sn) = 94$ (**M**)[g,j]
$C-CH_2-C$	1.81 (**M**); 1.5−1.8 (**m**)[g,h]	$^{3}J(^{1}H-^{119/117}Sn) \sim 145$ (**M**)[g,j,k]
CH_2N	2.47 (**M**)[i]	
CH_3N	2.35 (**M**); 2.30, 2.13 (**m**)[g]	
	^{13}C NMR (303 K; CD_2Cl_2)	
CH_2Sn	17.5	$^{1}J(^{13}C-^{119/117}Sn) = 1016/967$
$C-CH_2-C$	21.5	$^{2}J(^{13}C-^{119/117}Sn) = 50$[l]
CH_2N	60.5	$^{3}J(^{13}C-^{119/117}Sn) = 154$[l]
CH_3N	45.2	$^{1}J(^{13}C-^{15}N) \sim 154$
	^{13}C NMR (213 K; CD_2Cl_2)	
CH_2Sn	16.9 (**M**)	$^{1}J(^{13}C-^{119/117}Sn) = 1060/1010$ (**M**)
		$^{2}J(^{13}C-^{19}F) = 64$ (**M**)
	18.0 (**m**)	$^{1}J(^{13}C-^{119/117}Sn) = 940/900$ (**m**)
		$^{2}J(^{13}C-^{19}F) = 32$ (**m**)
$C-CH_2-C$	21.4 (**M**), 21.8 (**m**)	$^{2}J(^{13}C-^{119/117}Sn) = 50$ (**M**), 47 (**m**)[l]
CH_2N	60.3 (**M**), 59.5 (**m**)	$^{3}J(^{13}C-^{119/117}Sn) = 83$ (**M**), 67 (**m**)[l]
CH_3N	45.2 (**M**)	$^{1}J(^{13}C-^{15}N) \sim 142$
	44.1, 46.4 (**m**)	
	^{13}C CP/MAS NMR (303 K)	
CH_2Sn	18.8	$^{1}J(^{13}C-^{119/117}Sn) = 1030$[l]
$C-CH_2-C$	21.9	
CH_2N	60.1	
CH_3N	45.4, 44.3	

[a] ^{1}H and ^{13}C chemical shifts in ppm referenced to TMS from residual ^{1}H and $^{13}C-^{2}H$ solvent resonances, respectively. Coupling constants in Hz. [b] Unresolved broad multiplets. [c] $^{n}J(^{1}H-^{119}Sn)$ coupling constants determined from correlation doublets in the 1D $^{1}H-^{119}Sn$ HMQC spectrum. [d] No 1D $^{1}H-^{119}Sn$ HMQC correlation observed. [e] Broad singlet. [f] Maximum value, as assessed from unresolved $^{1}H-^{119}Sn$ HMQC correlation doublet. [g] $^{3}J(^{1}H-^{119}Sn)$ coupling pathway: $^{1}H-C-N \rightarrow {}^{119}Sn$. [h] **M** = major species; **m** = minor species. [i] Complex, broad pattern for minor species **m**. [j] Broad pattern for minor species **m** hidden under ^{1}H CH_3N resonance. [k] $^{n}J(^{1}H-^{119}Sn)$ coupling invisible for **m**. [l] Coupling satellites in partial overlap with resonances of **m**. [m] Unresolved $^{n}J(^{13}C-^{119}Sn)$ and $^{n}J(^{13}C-^{117}Sn)$ coupling satellites.

Table 4. ^{119}Sn and ^{19}F NMR Data for $[Me_2N(CH_2)_3]_2SnF_2\cdot 2H_2O$[a] (3a)

exptl conditions	chem shift	$^{1}J(^{119}Sn-^{19}F)$
303 K; solid state	$\delta(^{117}Sn)$[a] = −303.3 (t)	2720[b]
333 K; CCl_4/C_6D_6 (20 mg/0.5 mL)	$\delta(^{119}Sn)$[c] = −295.5 (s)	
303 K; CCl_4/C_6D_6 (20 mg/0.5 mL)	$\delta(^{119}Sn)$ = −292.1 (bs)[d]	
303 K; C_5D_5N (20 mg/0.5 mL)	$\delta(^{119}Sn)$ = −295 (bs)[d]	
303 K; CD_2Cl_2 (95 mg/0.5 mL)	$\delta(^{119}Sn)$ = −292.0 (bt)[e]	2782
303 K; CD_2Cl_2 (20 mg/0.5 mL)	$\delta(^{119}Sn)$ = −292 ± 3 (bt)[f]	*ca.* 2700−2800
223 K; CD_2Cl_2 (20 mg/0.5 mL)	$\delta(^{119}Sn)$ = −293.1 (t) (**M** 81%)[g]	2795
	$\delta(^{19}F)$[h] = −121.1	2782/2658[b]
	$\delta(^{119}Sn)$ = −283.3 (t) (**m** 19%)[g]	2688
	$\delta(^{19}F)$ = −150.2	2688/2566[b]

[a] Chemical shift data in ppm and $^{1}J(^{119}Sn-^{19}F)$ coupling constants in Hz. Coupling multiplet abbreviations: s = singlet; bs = broad singlet; t = triplet; bt = broad triplet; dt = doublet of triplets. In the solid state, ^{117}Sn NMR data acquisition referenced to (c-Hex)$_4$Sn. [b] $^{1}J(^{117}Sn-^{19}F)$. [c] ^{119}Sn resonances were referenced to the absolute frequency of Me_4Sn [$\Xi(^{119}Sn) = 37.290\,665$ MHz]. [d] Line width *ca.* 2400 Hz in CCl_4/C_6D_6, 5000 Hz in C_5D_5N. [e] Line width *ca.* 1800 Hz. [f] Very noisy spectrum; line width *ca.* 1700−1800 Hz. [g] **M** = major species and **m** = minor species with approximate relative populations in %. [h] ^{19}F resonances were referenced to the absolute frequency of Me_4Sn [$\Xi(^{19}F) = 94.094\,003$ MHz].

in the crystalline state. The $^{1}J(^{13}C-^{119/117}Sn)$ coupling constants of 940/900 Hz for the minor species **m** are somewhat lower. While absent in the fast-exchange ^{13}C spectra, $^{2}J(^{13}C-^{19}F)$ coupling triplets are observable for the slow-exchange ^{13}C resonances of the CH_2Sn moieties of both species with different $^{2}J(^{13}C-^{19}F)$ coupling constants of 64 Hz for **M** and 32 Hz for **m**. Hence, the exchange phenomenon occurs with loss of the $^{2}J(^{13}C-^{19}F)$ coupling on the ^{13}C NMR time scale at room temperature, that is, with intermolecular fluoride exchange. A single low-temperature ^{13}C *N*-methyl resonance is observed for **M** in agreement with its *all-trans* geometry observed in the crystalline state. The minor species **m** exhibits a pair of equally intense such resonances suggesting a chiral geometry.

Solution ^{119}Sn and ^{19}F NMR data for compound **3a** are presented in Table 4, together with CP/MAS ^{117}Sn data for solid **3a**. The ^{119}Sn pattern is a broad $^{1}J(^{119}Sn-^{19}F)$ triplet at room temperature in CD_2Cl_2 and a broad singlet in C_5D_5N (line width *ca.* 5000 Hz) and in CCl_4/C_6D_6 (line width *ca.* 2400 Hz). This indicates the intermolecular fluoride exchange rate to be solvent dependent and to increase in the order $CD_2Cl_2 < C_5D_5N < CCl_4$. At 333 K, the line width of the 119Sn resonance is less than 800 Hz in CCl_4/C_6D_6 indicating fast fluoride exchange on the ^{119}Sn NMR time scale ($k \gg 2800$ Hz, the order of magnitude of the $^{1}J(^{119}Sn-^{19}F)$ coupling constant). The loss of $^{1}J(^{119}Sn-^{19}F)$ coupling in CCl_4/C_6D_6 is reversible, as evaporating this solvent and

Table 5. Predicted NMR Patterns for the Possible Isomers of $[Me_2N(CH_2)_3]_2SnF_2$·$2H_2O$ (3a)

isomer	coupling pattern $^1J(^{119}Sn-^{19}F)$	coupling pattern $^2J(^{13}C-^{19}F)$	no. of ^{13}C N-methyl resonances
FtCt = major species **M**	triplet	triplet	1
FtCc	triplet	triplet	1
FcCcNt	triplet	doublet of doublets	2
FcCcNc	doublet of doublets	two doublets of doublets	4
FcCt = minor species **m**	triplet	triplet	2

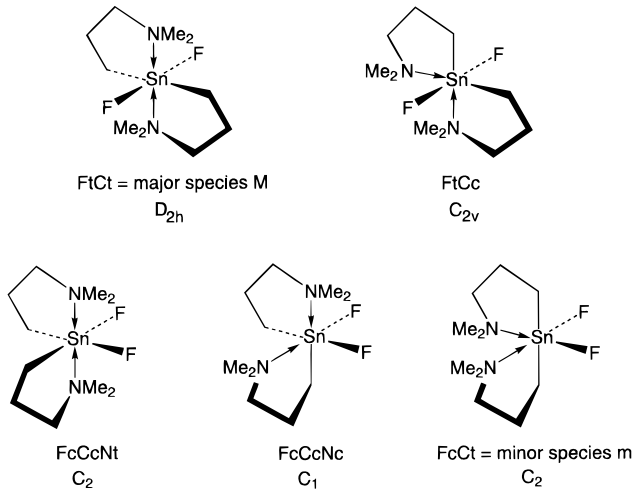

Figure 3. Possible isomers, with symmetry point group, assuming a distorted octahedral geometry for $[Me_2N(CH_2)_3]_2SnF_2$, as deduced from X-ray data. The isomer symbols refer to the configuration, *cis* or *trans*, for alike atoms. For instance, FcCcNt means that the F atoms have a *cis* arrangement, the C atoms have a *cis* arrangement, and the N atoms have a *trans* arrangement.

redissolving the sample in CD_2Cl_2 restores the characteristic broad triplet observed at room temperature.

The insensitivity of the ^{119}Sn chemical shift to solvent, temperature, and solution concentration, as well as the similar solid-state ^{117}Sn chemical shift, indicates comparable coordination features around tin in the solution and solid states. No coordination expansion in the presence of nucleophilic solvents is evidenced, indicating a very stable coordinating sphere, despite the intermolecular fluoride exchange. The absence of concentration effect on the ^{119}Sn chemical shift favors a dissociative rather than an associative mechanism for the intermolecular fluoride exchange.

At 223 K in CD_2Cl_2, the ^{119}Sn spectrum consists of two sharp $^1J(^{119}Sn-^{19}F)$ triplets in the approximate intensity ratio 20/80, centered at −283.3 and −293.1 ppm and assigned to the minor species **m** and the major species **M**, respectively. Their $^1J(^{119}Sn-^{19}F)$ coupling constants are very similar as is that of the solid-state species (Table 4). The ^{19}F NMR data essentially confirm the conclusions from the ^{119}Sn NMR data, with a very broad resonance without $^1J(^{19}F-^{119/117}Sn)$ coupling satellites at room temperature. The small inconsistency between the $^1J(^{119}Sn-^{19}F)$ values from ^{119}Sn and ^{19}F NMR data at low temperature is artifactual since the $^1J(^{117}Sn-^{19}F)$ coupling is unambiguously evidenced by a $2D^{19}F-^{117}Sn$ HMQC correlation spectrum, recorded according to Berger.[13a]

Identification of the Solution Isomers. Figure 3 shows the a priori possible isomers for **3a** in solution, assuming a distorted octahedral molecular skeleton, as observed in the crystalline state. Table 5 gives the predicted NMR spectral patterns for each of these isomers. The high similarity between solid- and solution-state values for the key NMR parameters, mainly the ^{119}Sn chemical shift, as well as the $^1J(^{119}Sn-^{19}F)$ and $^1J(^{13}C-^{119}Sn)$ coupling constants, identifies the major species **M** in solution as the *all-trans*-configured structure (FtCt) observed in the crystalline state. The data are in agreement with its D_{2h} symmetry in solution. The *N*-methyl resonance duplication in the ^{13}C CP/MAS spectrum of **3a** is assigned to unidentified crystal packing effects.

The structure of **m** is unambiguously that of the FcCt isomer (Table 5 and Figure 3). Thus, the pair of *N*-methyl resonances in the low-temperature ^{13}C spectrum rule out the isomers with the fluorine atoms in *trans* configuration (FtCt and FtCc: one single resonance predicted) as well as the asymmetric *all-cis* isomer (FcCcNc: four *N*-methyl resonances predicted). Among the two possible isomers left, the isomer with two NMe_2 moieties in *trans* (FcCcNt) is ruled out on the basis of the expected $^2J(^{13}C-^{19}F)$ doublet of doublets, in disagreement with the observed triplet.

This finding reinforces indirectly the assignment of the major solution species **M** to isomer FtCt. Indeed, the two observed isomers have in common their carbon atoms in *trans* configuration, which appears to be the only stable one. Such a *trans* configuration for the organic R moieties in six- or seven-coordinate diorganotin compounds, in particular those with distorted octahedral geometry of the type $R_2SnX_2D_2$, where X is an electronegative or nucleophilic atom or atom group and D is a coordinating ligand causing hypervalency at tin, is well established[1,3,4,5,10e,29] and in agreement with the polarity rule of Bent.[30a] We therefore rule out that the C_{2v} isomer FtCc might be the major species **M**.

Isomerization Mode. 1D $^1H-^{119}Sn$ HMQC Experiments. Rearrangements in hypervalent organotin compounds by a dissociation−reassociation mechanism involving a $Me_2N\rightarrow Sn$ moiety are well-known.[1b,31] In addition, a similar mechanism was proposed for six-coordinate silicon complexes containing likewise rearranging $Me_2N\rightarrow Si$ moieties.[32] A recent six-coordinate silicon complex reported by Corriu et al.[32b] isomerizes via a $Si\leftarrow NMe_2$ dissociation−reassociation mechanism rather than by Si−F bond rupture. The main evidence was maintenance of $^1J(^{29}Si-^{19}F)$ coupling multiplets throughout the whole temperature range. It is therefore

(30) (a) Bent, H. A. *Chem. Rev.* **1961**, *61*, 275. (b) Van Koten, G.; Jastrzebski, J. T. B. H.; Noltes, J. G.; Spek, A. L.; Schoone, J. C. *J. Organomet. Chem.* **1978**, *148*, 233.

(31) (a) Wynants, C.; Van Binst, G.; Mügge, C.; Jurkschat, K.; Tzschach, A.; Pepermans, H.; Gielen, M.; Willem, R. *Organometallics* **1985**, *4*, 1906. (b) Jurkschat, K.; Schilling, J.; Mügge, C.; Tzschach, A.; Piret-Meunier, J.; Van Meerssche, M.; Gielen, M.; Willem, R. *Organometallics* **1988**, *7*, 38. (c) Jurkschat, K.; Tzschach, A.; Mügge, C.; Piret-Meunier, J.; Van Meerssche, M.; Van Binst, G.; Wynants, C.; Gielen, M.; Willem, R. *Organometallics* **1988**, *7*, 593.

(32) (a) Kalikhman, I.; Kost, D.; Raban, M. *J. Chem. Soc., Chem. Commun.* **1995**, 1253. (b) Carre, F.; Chuit, C.; Corriu, R. J. P.; Fanta, A.; Mehdi, A.; Reye, C. *Organometallics* **1995**, *14*, 194. (c) Huheey, J. E. *Inorganic Chemistry*; de Gruyter: Berlin, 1988; p 1071.

Table 6. ^{1}H, ^{13}C, ^{19}F, and ^{119}Sn NMR Data for $\{[Me_2(ClCH_2)N^+(CH_2)_3][Me_2N(CH_2)_3]SnF_3^-\}\cdot H_2O$ (3b)[a,l]

moieties	chem shifts (integration) (pattern)	coupling constants
	^{1}H NMR (313 K)	
$N^+\sim CH_2Sn$	1.13 (2H) (t)	$^{3}J(^{1}H-^{1}H) = 7.5$; $^{2}J(^{1}H-^{119/117}Sn)^b \sim 80$
$N\sim CH_2Sn$	1.07 (2H) (t)	$^{3}J(^{1}H-^{1}H) = 7.5$; $^{2}J(^{1}H-^{119/117}Sn)^b \sim 80$
$N-C-CH_2$	1.85 (2H) (tt)	$^{3}J(^{1}H-^{1}H) = 7$ and 7; $^{3}J(^{1}H-^{119/117}Sn)^b \sim 125$
N^+-C-CH_2	2.17 (2H) (m)	$^{3}J(^{1}H-^{119/117}Sn)^b \sim 100$
$N-CH_2$	2.46 (2H) (bt)	$^{3}J(^{1}H-^{1}H) = 7$
N^+-CH_2	3.5 −3.6 (2H) (m)	
$N-CH_3$	2.38 (6H) (s)	
N^+-CH_3	3.22 (>6H) (s)[c]	
"free" HOH	∼4.9 (>2H) (bs)[d]	
N^+-CH_2-Cl	5.25 (2H) (s)[e]	
	^{13}C NMR (303 K)	
$N\sim CH_2Sn$	21.3	$^{1}J(^{13}C-^{119/117}Sn) = 1135/1083$
$N^+\sim CH_2Sn$	21.0	$^{1}J(^{13}C-^{119/117}Sn) = 1131/1083$
N^+-C-CH_2	20.0	$^{2}J(^{13}C-^{119/117}Sn) = 38$[f]
$N-C-CH_2$	21.9	$^{2}J(^{13}C-^{119/117}Sn) = 51$[f]
N^+-CH_2	67.1	$^{3}J(^{13}C-^{119/117}Sn) = 120$[f]
$N-CH_2$	61.6	$^{3}J(^{13}C-^{119/117}Sn) = 86$[f]
N^+-CH_3	49.9	
$N-CH_3$	45.6	
N^+-CH_2Cl	70.0	
	^{19}F	
303 K	−129.8 (bs)	
	−143.0 (bs)	
273 K	−128.9 (bs)	
	−142.3 (s)	$^{1}J(^{19}F-^{119/117}Sn)$[g] = 2905
193 K	−127.7 (d)	$^{1}J(^{19}F-^{119/117}Sn)$[g] *ca.* 2970;[h] $^{2}J(^{19}F-^{19}F) = 28$[i]
	−139.2 (t)	$^{1}J(^{19}F-^{119/117}Sn)$[g] *ca.* 2640;[h] $^{2}J(^{19}F-^{19}F) = 30$[i]
	^{119}Sn	
303 K	−377 (bd)[j]	$^{1}J(^{19}F-^{119}Sn) = 2850 \pm 50$[k]
193 K	−374 (dt)	$^{1}J(^{19}F-^{119}Sn) = 2970; 2663$
	−457 (bt)	$^{1}J(^{19}F-^{119}Sn) = 2720 \pm 20$[k]

[a] Solvent: CD_3OD (referencing: see legends of Tables 3 and 4). [b] Unresolved and broad $^{n}J(^{1}H-^{119}Sn)$ and $^{n}J(^{1}H-^{117}Sn)$ satellites. [c] Overlapping with residual CHD_2OD signal. [d] "Free OH" = resonance of water protons averaging with residual CD_3OH resonance. [e] N^+-CH_2-Cl = function generated from reaction with CH_2Cl_2; see text. [f] Unresolved $^{n}J(^{13}C-^{119}Sn)$ and $^{n}J(^{13}C-^{117}Sn)$ satellites. [g] Unresolved $^{1}J(^{19}F-^{119}Sn)$ and $^{1}J(^{19}F-^{117}Sn)$ satellites. [h] Estimation, because of broad and overlapping multiplet $^{1}J(^{19}F-^{119}Sn)$ and $^{1}J(^{19}F-^{117}Sn)$ satellites. [i] Error *ca.* 2 Hz. [j] Line width *ca.* 2000 Hz. [k] Low signal-to-noise ratio. [l] Abbreviations: s = singlet; bs = broad singlet; bd = broad doublet; bt = broad triplet; d = doublet; dd = doublet of doublets; dt = doublet of triplets; m = undefined multiplet or complex pattern; t = triplet; refer to the pattern of the parent resonances.

somewhat unexpected that an intermolecular fluoride exchange is observed in the present six-coordinate $R_2SnF_2N_2$ system, where a similar dissociation−reassociation mechanism could have reasonably been expected.

In order to assess whether a rearrangement by a $Me_2N\rightarrow Sn$ dissociation−reassociation mechanism can occur simultaneously to the intermolecular fluoride exchange or not, we performed gradient-enhanced [10a,10e] 1D $^{1}H-^{119}Sn$ HMQC[12,33] experiments on the CCl_4/C_6D_6 solution of compound **3a** at 333 K. The CCl_4/C_6D_6 solution of compound **3a** at 333 K was chosen because, as shown above, the $^{1}J(^{119}Sn-^{19}F)$ coupling is lost at such a temperature on the ^{119}Sn NMR time scale, indicating a rate constant exceeding 2800 s^{-1} for the dissociative fluoride exchange.

Figure 2 (top) shows the 1D gradient assisted $^{1}H-^{119}Sn$ HMQC spectrum obtained with a delay[10a,e,11] of 120 ms. This latter long delay makes optimally observable long-range $^{n}J(^{1}H-^{119}Sn)$ coupling constants of typically less than 10 Hz. This explains that the $^{n}J(^{1}H-^{119}Sn)$ HMQC correlations associated with the coupling satellites of the CH_2Sn and $C-CH_2-C$ resonances have low amplitudes, being observed optimally at much shorter delays (10−20 ms). The key point is that the

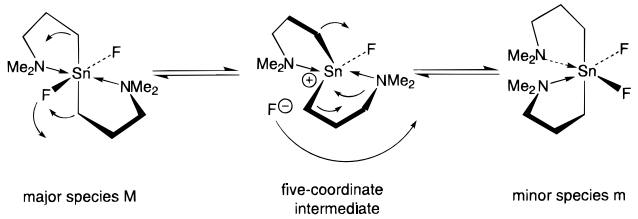

Figure 4. Isomerization through intermolecular fluoride exchange interconverting the major species **M** and the minor species **m** through a five-coordinate cationic intermediate.

$^{1}H-^{119}Sn$ HMQC spectrum displays an intense correlation of the ^{119}Sn nucleus with the *N*-methyl protons. This correlation arises essentially from the $^{3}J(^{1}H-C-N\rightarrow^{119}Sn)$ coupling pathway through the coordinative nitrogen-to-tin bond. The alternative $^{6}J(^{1}H-C-N-C-C-C-^{119}Sn)$ coupling pathway through the trimethylene chain is considered to have a lower contribution to the observed $^{1}H-^{119}Sn$ HMQC correlation. The absence of observable splitting for the $^{3}J(^{1}H-C-N\rightarrow^{119}Sn)$ coupling in the $^{1}H-^{119}Sn$ HMQC correlation signal of the *N*-methyl group indicates the coupling to be no more than 2 Hz, as is common for couplings through coordinative Lewis donor to tin bonds.[10e,12,29,33] These data show the $Me_2N\rightarrow Sn$ bonds in **3a** to have at least a lifetime of 120 ms, the time needed in the pulse sequence to develop the multiple quantum coherence

(33) Biesemans, M.; Willem, R.; Damoun, S.; Geerlings, P.; Lahcini, M.; Jaumier, P.; Jousseaume, B. *Organometallics* **1996**, *15*, 2237.

necessary for the observation of the $^1H-^{119}Sn$ HMQC correlation. With a shorter lifetime, the correlation would collapse. This minimum lifetime establishes the *upper limit* to the rate constant for dissociation−reassociation of the $Me_2N\rightarrow Sn$ bonds at about 8 s^{-1}, showing that, if the latter mechanism exists at all, it must be at least 350 times slower than the intermolecular fluoride exchange, the *minimum* rate constant estimated above at least 2800 s^{-1} at 333 K in CCl_4/C_6D_6.

A $^1H-^{119}Sn$ HMQC spectrum intrinsically edits only that species where a $^nJ(^1H-^{119}Sn)$ coupling pathway does exist, "spoiling away" any other species where such a coupling is not observable. This occurs even if there is an exchange between species with and without couplings, which is moderate to fast on the ^1H NMR time scale of a standard 1D ^1H spectrum. For this reason, dissociation−reassociation of the $Me_2N\rightarrow Sn$ bond cannot be ruled out, the time scale of the $^1H-^{119}Sn$ HMQC experiment allowing, however, to determine its maximum rate constant at 8 s^{-1} as outlined above.

The dissociative intermolecular fluoride exchange mechanism proposed from these observations is presented in Figure 4. The cationic intermediate is assumed to have a distorted five-coordinate trigonal bipyramidal geometry, with the fluorine and the two carbon atoms in equatorial positions and the two coordinative nitrogen tin bonds occupying the apical positions.[30a] Only relatively low-amplitude motions are needed to convert the five-coordinate intermediate to any of the two possible six-coordinate ones. It is reasonable to assume a higher Lewis acidity and hence stronger $Me_2N\rightarrow Sn$ bonds in this five-coordinate intermediate than in the six-coordinate species. This is in accordance with the slower dissociation−reassociation mechanism. Ionic intramolecular pentacoordinated organotin halides have been described in the literature.[1d,30b]

In conclusion, we do not exclude that a $Me_2N\rightarrow Sn$ dissociation−reassociation mechanism is operative but we can state that it is at least 350 times slower than fluorine exchange by Sn−F bond rupture. It is quite acceptable that there is a difference in the exchange phenomena between the tin and silicon complexes. Thus, the Si-F bond is very strong,[32c] which overcomes energy gain by nitrogen chelation, as illustrated by Corriu's complex.[32b] The Sn−F bond, in contrast, is weaker,[32c] so the nitrogen chelation is dominant.

Reaction of $[Me_2N(CH_2)_3]_2SnF_2 \cdot 2H_2O$ (3a) with Fluoride. The reaction of **3a** with tetrabutylammonium fluoride in dichloromethane afforded a colorless amorphous precipitate hereafter referred to as **3b**.

An overview of the NMR data obtained from a CD_3OD solution of **3b** is provided in Table 6.

The ^1H and ^{13}C spectra which are essentially temperature independent confirm the total absence of Bu_4N^+ cations in **3b**. When compared with **3a**, the NMR spectra at room temperature of **3b** reveal duplication of all the ^1H and ^{13}C resonances. The high-frequency shifts of the ^1H and ^{13}C resonances of the $N-CH_2$ and the $N-CH_3$ groups of one $(CH_3)_2N(CH_2)_3$ moiety with respect to the other one suggest quaternization of one of the nitrogen atoms.

Interestingly, the ^1H NMR spectrum exhibits two additional resonances at 4.90 and 5.25 ppm, while the ^{13}C spectrum shows an unexpected ninth resonance at 70.0 ppm. The ^1H signal at 4.90 ppm is assigned to exchangeable hydroxylic protons, merged with the resonance of residual CD_3OH, since addition of a few microliters of either CH_3OH or H_2O causes this resonance to increase in intensity. The other singlet at 5.25 ppm remains narrow and keeps a constant integrated area (2 H).

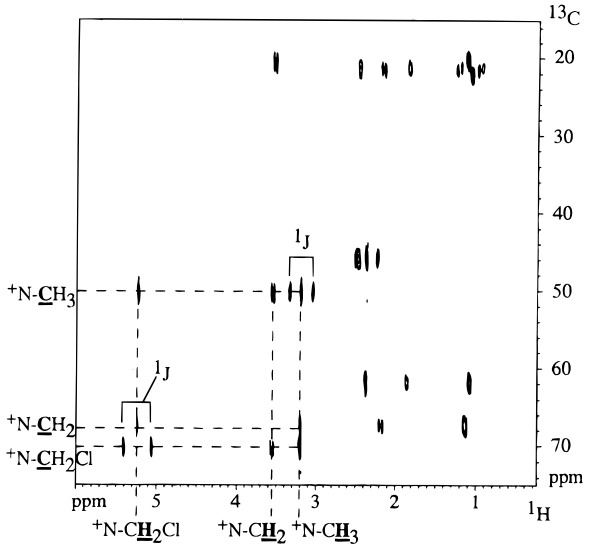

Figure 5. Two-dimensional $^1H-^{13}C$ HMBC spectrum of compound **3b**. The dotted line grid evidences the mutual $^1H-^{13}C$ HMBC correlations between the ^1H and ^{13}C resonances of the $^+N-CH_2Cl$, $^+N-CH_2^-$ and $^+N-CH_3$ moieties, resulting from $^3J(^1H-^{13}C)$ coupling pathways and demonstrating the existence of the $(CH_3)_2(CH_2Cl)N^+-(CH_2)_3-$ moiety in compound **3b**. ^1J represents the $^1J(^1H-^{13}C)$ coupling satellite pair associated with the residual $^1J(^1H-^{13}C)$ cross-peak doublets of the $^+N-CH_2Cl$ and $^+N-CH_3$ HMQC spectrum which are not entirely suppressed in the HMBC spectrum, because of a slight mismatch of the low-pass filter tuned to the $^1J(^1H-^{13}C)$ couplings of the chain CH_2 group resonances.[10,11] Note also that the cross-peak associated with the $^3J(^1H-^{13}C)$ coupling between the protons of one CH_3 group and the ^{13}C nucleus of the other CH_3 group within the $(CH_3)_2N^+(CH_2Cl)$ moiety is likewise observed in the middle of the residual $^1J(^1H-^{13}C)$ doublet of the $^+N-CH_3$ group. The organic chain specific assignments of the ^1H and ^{13}C resonances presented in Table 6 have been determined from this HMBC spectrum.

A gradient-assisted[10] $^1H-^{13}C$ HMQC[11a] experiment reveals that the ^1H singlet at 5.25 ppm and the ^{13}C resonance at 70.0 ppm are correlated by a $^1J(^1H-^{13}C)$ coupling of 173 Hz. A ^{13}C DEPT-135 spectrum reveals this pair of correlated resonances to arise from a CH_2 moiety. The latter does not originate from CH_2Cl_2, as addition of a few microliters of CH_2Cl_2 to the solution of **3b** provides the additional ^1H and ^{13}C resonances expected.

A 2D $^1H-^{13}C$ HMBC[11b] spectrum (Figure 5) reveals this pair of $^1H-^{13}C$ resonances to correlate with the *N*-methyl and *N*-methylene resonances of the ammonium moiety. This is firm evidence for the existence in **3b** of a moiety of the type $-CH_2-[(CH_3)_2N^+]-CH_2Cl$, as further evidenced by elemental analysis and electrospray mass spectrometry.

The ^{19}F spectrum at room temperature exhibits two different broad resonances. Cooling to 273 K confirms the presence of two signals in the ratio 2:1. The high-frequency one associated with two fluorine atoms is a broad singlet, without visible $^1J(^{19}F-^{119/117}Sn)$ satellites. The low-frequency one, associated with the third fluo-

Scheme 2

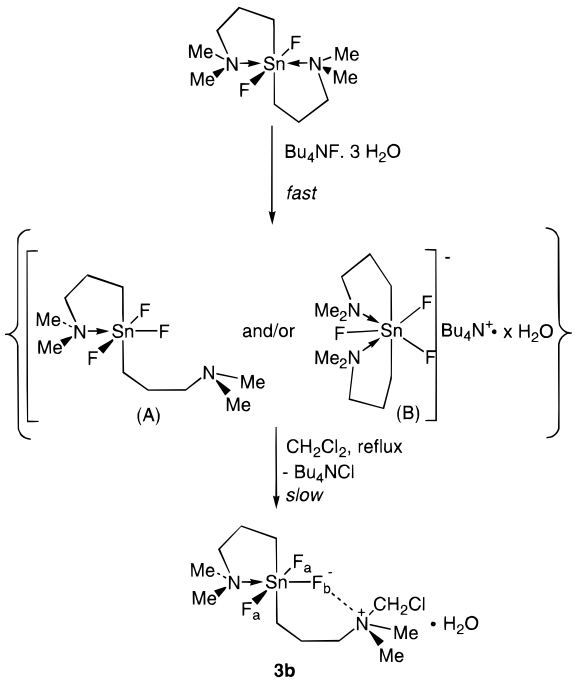

rine atom, is now, in contrast, narrowed out with respect to room temperature and reveals unresolved $^1J(^{19}F-^{119/117}Sn)$ satellites. At 193 K both resonances cause further narrowing to a $^2J(^{19}F-^{19}F)$ triplet and a $^2J(^{19}F-^{19}F)$ doublet at low and high frequency, respectively. Overlapping $^1J(^{19}F-^{119/117}Sn)$ multiplet satellites are also visible for both ^{19}F resonance sets. Cooling is accompanied by only a slight high frequency shift of both ^{19}F resonance sets (Table 6).

The ^{119}Sn spectrum at room temperature appears as an extremely broad and noisy doublet. At 193 K this pattern narrows out into a doublet of triplets with two slightly different $^1J(^{19}F-^{119}Sn)$ coupling constants. The ^{119}Sn chemical shift is independent of the temperature (see Table 6).

The CP-MAS ^{117}Sn spectrum reveals extremely complicated chemical shift anisotropy patterns, precluding the identification of a clear multiplet. However, spectra at three different spinning rates reveal spinning rate independent resonances, overlapping with other spinning rate dependent ones around −310, −340, −370, and −400 ppm, suggesting the presence of a four-line multiplet centered at *ca.* −355 ppm.

These data enable a structure shown in Scheme 2 to be proposed for the coordination sphere around the tin atom in **3b**.

It consists of a distorted octahedral geometry with the two Sn−C bonds in mutual trans configuration, as supported by the high $^1J(^{13}C-^{119}Sn)$ coupling constants. The *N*,*N*-dimethylamino group of one organic moiety is quaternized as discussed above, the other one has its nitrogen coordinating the tin atom, in agreement with the signal duplication observed in the ^1H and ^{13}C spectra and associated high-frequency shifts of the relevant NCH_2 and NCH_3 resonances. It is likely that electrostatic attraction between the quaternized nitrogen and fluoride F_b stabilizes a six-membered chelate.

The room-temperature ^{119}Sn and ^{19}F data indicate intermolecular, dissociative, fluoride exchange, as in **3a**. The low-temperature ^{119}Sn and ^{19}F patterns are in agreement with the proposed geometry around tin, as supported by the slightly different $^1J(^{19}F-^{119}Sn)$ coupling constants of 2970 and 2663 Hz as well as the $^2J(^{19}F-^{19}F)$ doublet and triplet in the ratio 2:1 for the two "F_a" (*cis* to coordinated nitrogen) and single "F_b" (*trans* to coordinated nitrogen) fluorine atoms, respectively. The intermediate temperature range (253−273 K) ^{19}F spectrum is in agreement with intermolecular exchange of the F_a atoms becoming fast but that of the F_b atom remaining slow on the observational ^{19}F NMR time scale.

However, in the room-temperature range, the slower intermolecular exchange of the F_b atom likewise becomes fast on the ^{19}F NMR time scale.

The reason for the unexpected formation of **3b** is not quite clear yet. It seems that the hepta- and/or hexacoordinate intermediates A and B (Scheme 2) formed from **3a** upon addition of fluoride exhibit a markedly enhanced nucleophilicity of the nitrogens. Such a behavior is unprecedented in organotin chemistry but resembles the enhanced basicity of nitrogen in Corriu's {2,6-bis[(dimethylamino)methyl]phenyl}bis(1,2-benzenediolato)silicate.[34]

Further studies on this subject are in progress.

Acknowledgment. Partial funding of this research by Contract ERBCHRX-CT94-0610 of the Human Capital & Mobility (HCM) Programme of the European Union is acknowledged (K.J., R.W.). K.J. thanks the German "Fonds der Chemischen Industrie" for support. The financial support of the Belgian National Science Foundation (FKFO, Grant NR 2.0094.94) and of the Belgian "Nationale Loterij" (Grant NR 9.0006.93) is also acknowledged (R.W., M.B.).

Supporting Information Available: Lists of all coordinates and *U* values, anisotropic displacement parameters, and all geometric data for **3a** and a stereoscopic view (SHELXTL-PLUS) of the unit cell of **3a** (6 pages). Ordering information is given on any current masthead page.

OM960895H

(34) Chuit, C.; Corriu, R. J. P.; Mehdi, A.; Reye, C. *Chem. Eur. J.* **1996**, *2*, 342.